Fourier transform second harmonic generation for high-resolution nonlinear spectroscopy

Kristensen, Mathias Hedegaard; Kristensen, Peter Kjær; Pedersen, Kjeld; Skovsen, Esben

Published in:
Optics Communications

DOI (link to publication from Publisher):
10.1016/j.optcom.2020.126593

Publication date:
2021

Document Version
Accepted author manuscript, peer reviewed version

Fourier Transform Second Harmonic Generation for High-Resolution Nonlinear Spectroscopy

Mathias Hedegaard Kristensen*, Peter Kjær Kristensen, Kjeld Pedersen, Esben Skovsen*

Department of Materials and Production, Section for Physics and Mechanics, Aalborg University, DK-9220 Aalborg East, Denmark

Abstract

In this communication we demonstrate a new characterization technique combining Fourier transform (FT) spectroscopy and second harmonic generation (SHG) that enables high spectral resolution with broadband femtosecond laser pulses. The strong and narrow exciton resonances of the wide band gap semiconductor ZnO were chosen for demonstrating the capabilities of the method. FT-SHG offers high reproducibility and high spectral resolution within the bandwidth of the input pulse.

Keywords: Nonlinear optics, Harmonic generation, Fourier transform, Spectroscopy

1. Introduction

During the last decades second-order nonlinear optical (NLO) processes have become essential tools within studies of semiconductor materials [1, 2, 3]. Second-order NLO processes have different selection rules from linear optics. This has led to a wealth of applications, where valuable information on inhomogeneous structures, surfaces, interfaces, and metamaterials has been obtained. Furthermore, the NLO techniques benefit from being contact-free, applicable for layers buried in transparent media, and generally non-destructive.

Fourier transform (FT) spectroscopy is a well-established technique applied in many different fields of science such as nuclear magnetic resonance (NMR) spectrometry, optical spectroscopy, and terahertz spectroscopy. [4, 5]

One of the inherent advantages of optical FT spectroscopy is the multiplex nature, i.e. all of the spectral components are measured simultaneously, known as Fellget's advantage [6], which increases the signal-to-noise ratio. This advantage cannot be exploited in the case of weak NLO signals, since detectors working in the UV range are dominated by shot noise, which equals the gain in signal-to-noise ratio. However, the single-shot feature of the technique using broadband femtosecond pulses is still beneficial in terms of scan duration. Connes' (the spectral accuracy) advantage [6] may be less well known. Nonetheless, it is very significant to the FT technique. The spectral sampling intervals are inversely proportional to the optical sampling intervals, wherefore the respective errors are directly coupled. The change in optical path difference can be tracked very precisely using the interference pattern of monochromatic light of a HeNe laser. By this approach the accuracy of the optical sampling intervals is entirely determined by the precision of the HeNe laser wavelength itself. Thus, FT spectroscopy measurements have a built-in calibration of the spectral axis giving the technique a very high spectral reproducibility. Finally, the FT approach has the advantage of practically unlimited spectral resolution. This is due to the fact that the resolution does not rely on the input pulse characteristics but is entirely determined by the maximum optical path difference of the interferometer. However, the FT method has primarily gained ground within infrared (IR) and terahertz spectroscopy. [5, 6, 7] Nevertheless, it has been demonstrated that ultrafast laser spectroscopy can take advantage of the benefits of the FT technique. This was accomplished by Bellini *et. al.* by the demonstration of Ramsey spectroscopy with femtosecond laser pulses [8] and most recently McGuire *et. al.* demonstrated IR-visible FT sum-frequency generation (FT-SFG) with femtosecond laser pulses, where the IR beam is modulated by an interferometer [9].

During recent years, more and more research groups have replaced their old nanosecond, picosecond, or 100 fs laser systems with modern ultrafast laser systems. The light pulses of the modern lasers are typically sub-40 fs and thus spectrally broader, which limits the achievable spectral resolution for conventional nonlinear spectroscopy.

In this communication, we present a new NLO technique combining second harmonic generation (SHG) and FT spectroscopy to circumvent this limit and give access to high spectral resolution with ultrafast laser pulses. Broadband femtosecond laser pulses are used to induce a polarization in a sample, whereupon the recorded interferogram of the response is Fourier transformed to acquire the spectral content.

An exhaustive theoretical and experimental study of the exciton resonances of the wide band gap hexagonal semiconductor ZnO in the range of 3.2 - 3.5 eV photon energy has previously been carried out by Lafrentz *et. al.* [10]. Strong crystallographic SHG signals were reported for parallel p-polarized fundamental and SHG light in transmission at a sample tem-

*Corresponding authors.

Email addresses: math@mp.aau.dk (Mathias Hedegaard Kristensen), es@mp.aau.dk (Esben Skovsen)

perature T of 1.6 K using a nanosecond-pulse-width laser with narrow spectral bandwidth. Several sharp lines were found in the exciton spectral range from 3.37 - 3.44 eV. The broadening of the excitons at temperatures exceeding 20 K was found to be almost homogeneous and linearly increasing with temperature. The peak intensity and the full width at half maximum (FWHM) of the X-line and the $1s_L(C)$ exciton change slower with temperature compared to the $2p_{x,y}(A)$ states [10]. Regarding our work, the X-line at 3.407 eV is pertinent for benchmarking the FT-SHG technique due to its strong and narrow characteristics.

We find that the exciton peak can be resolved if the FT technique is applied. Furthermore, the width of the exciton peak is found to be three times smaller using the FT technique in comparison to regular SHG experiments using 100-fs laser pulses.

2. Experimental Methods and Materials

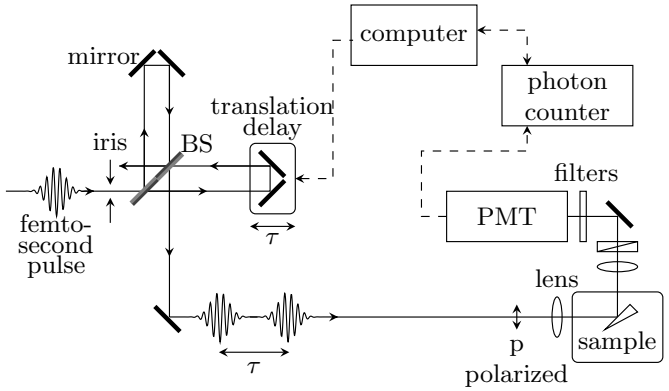

Figure 1: Illustration of the FT-SHG setup. BS, beam splitter; PMT, photomultiplier. For details see text.

The FT-SHG setup is illustrated in Fig. 1. A beam of laser pulses (725 nm center wavelength, 10 nm FWHM , ∼100 fs pulse width, 600 mW average power, and 80 MHz repetition rate) generated by a Ti:sapphire Tsunami femtosecond laser from Spectra-Physics, was sent through a home-built Michelson interferometer. A specially designed dielectric 50/50 beam splitter from Femto Optics obviates the need of an additional compensation plate, since each surface has a coated and uncoated section. The optical delay was established by a N-565 PiezoWalk linear stage and the appertaining E-861 controller from Physik Instrumente (PI). The N-565 stage utilizes an optical nanometrology encoder to ensure a stable, smooth, and precise linear translation of suitable length (13 mm travel range, 3 nm minimum incremental motion, and 0.5 nm resolution). Additionally, the interferometric encoder ensures the reproducibility of the spectral axis through Connes' advantage. The field leaving the Michelson interferometer, $\mathbf{E}_\mathrm{M}$, was a superposition of two short pulses separated in time. Next, the beam was incident at 45° upon the sample mounted in a cryostat at a temperature of approx. 60 K. Prior to the sample, a long pass filter was inserted to block any previously generated SH light. The ZnO sample was cut from a (1000)-oriented ZnO single crystal and polished into a 5° wedge such that the back reflection can be avoided and the reflection from the first interface can be isolated in order to avoid Maker fringe effects [11]. The reflected SHG originates from a thin surface layer with a thickness of the order of the wavelength [12]. The signal is therefore small compared to the transmitted signal, but there is only a small effect of the linear absorption on the SH signal. It is thus expected that the spectra directly demonstrate excitonic resonances near the ZnO bandgap.

The SH signal generated at the sample was reflected into a photomultiplier tube (PMT) with proper band pass filters attached to block the fundamental and third harmonic, while transmitting the second harmonic. The signal detected by the PMT was recorded by a Stanford Research Systems SR400 gated photon counter. The SHG measured in reflection from a quartz crystal wedge was used to normalize the ZnO signal. Furthermore, the measurements were carried out for a p-to-p polarization combination. The signal was recorded by the computer as the optical delay was varied in a step-scan mode.

The output of the Michelson interferometer $\mathbf{E}_\mathrm{M}(t,\tau)$ is the sum of two replicas of the input fields $\mathbf{E}(t) + \mathbf{E}(t-\tau)$, where

$$\mathbf{E}(t) = \int_{-\infty}^{\infty} \tilde{\mathbf{E}}(\omega) \exp[-i\omega t]\, \mathrm{d}\omega, \tag{1}$$

and $\tilde{\mathbf{E}}$ is the Fourier Transform of $\mathbf{E}(t)$, and similar for the delayed replica $\mathbf{E}(t-\tau)$. Upon incidence on the sample the electric field induces a nonlinear polarization $\mathbf{P}^{(2)} = \epsilon_0 \chi^{(2)} \mathbf{E}^2$, where $\chi^{(2)}$ is the nonlinear susceptibility tensor. Hence, the reflected SHG field can be written as

$$\mathbf{E}_\mathrm{SHG}(\tau) \propto \chi^{(2)} \mathbf{E}_\mathrm{M}^2(\tau) \tag{2}$$

The SHG signal of a single pulse measured by the photomultiplier is given by

$$I_\mathrm{SHG}(\tau) \propto \int_{-\infty}^{\infty} |\mathbf{E}_\mathrm{SHG}(t,\tau)|^2\, \mathrm{d}t \propto \int_{-\infty}^{\infty} |\chi^{(2)}|^2 |\mathbf{E}_\mathrm{M}^2(t,\tau)|^2\, \mathrm{d}t. \tag{3}$$

For $\chi^{(2)} = 1$ this is the second order interferometric autocorrelation of $\mathbf{E}(t)$ and $\mathbf{E}(t-\tau)$. Finally, the spectrum can be achieved by Fourier transforming the measured SHG signal, i.e.

$$I_\mathrm{SHG}(\omega) = \mathcal{F}\left(I_\mathrm{SHG}(\tau)\right) \propto |\chi^{(2)}(\omega)|^2 |\tilde{\mathbf{E}}_\mathrm{M}^2(\omega)|^2 \tag{4}$$

3. Results and Discussion

Fig. 2 shows the SHG interferogram of the ZnO crystal wedge. The interferogram was recorded by scanning the optical delay by roughly 3.33 ps in 1.67 fs increments integrating for 500 ms. The magnified tail of the interferogram shown in the inset of Fig. 2 reveals a long-lasting oscillation, which indicates narrow spectral features in the signal.

Prior to the Fourier transform the recorded interferograms were baseline corrected and multiplied by an apodization function. Various apodization functions including triangular, Blackman-Harris, and Hanning were tested, however, no pronounced differences were seen in the region of interest. Therefore, the triangular apodization function was used onward. Subsequently, the data were zero padded to the next power of twice

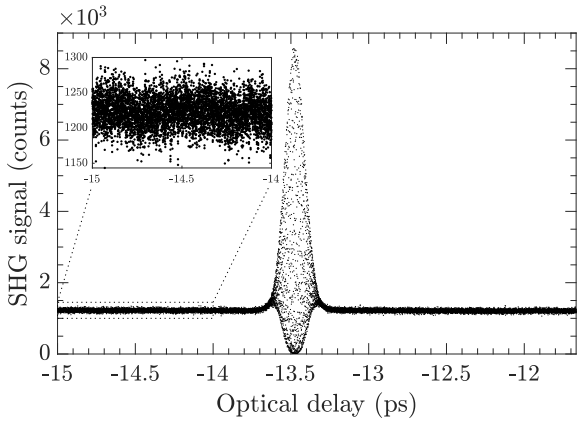

Figure 2: SHG interferogram of the wedged ZnO crystal sample.

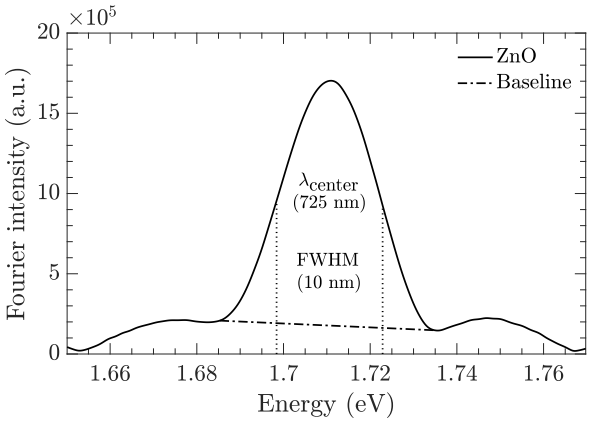

Figure 4: Zoom-in of the fundamental peak seen in Fig. 3.

its length. Finally, in accordance to common practice [6], the signal was shifted about the maximum signal to reference the signal as close to zero phase as possible before being Fourier transformed.

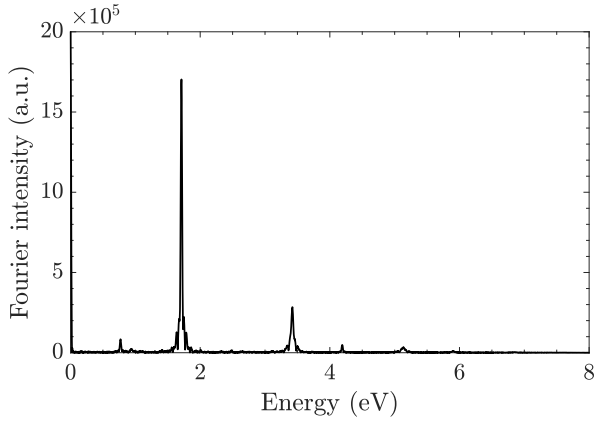

Figure 3: The Fourier spectrum of the SHG interferogram shown in Fig. 2 cropped to 8 eV.

The Fourier spectrum corresponding to the interferogram shown in Fig. 2 of the ZnO crystal wedge is seen in Fig. 3. The 3.33 ps optical delay in 1.67 fs increments transform to a spectral resolution of 1.2 meV and a 12.4 eV spectral range. However, the Fourier spectrum in Fig. 3 has been cropped, since no signal nor aliasing are present above 8 eV. Distinct peaks of the Fourier intensity in Fig. 3 are seen around 1.71 and 3.42 eV corresponding to the fundamental and SHG energies of 725 nm light, respectively. The fundamental peak is an inherent part of the Fourier transformed signal even though only the SHG light reached the detector, while the incident near IR was completely blocked by filters. This is due to the interferometric nature of the probe signal. Fig. 4 shows a zoom-in of the fundamental peak. The central energy of the peak translates to a center wavelength of 725 nm while the FWHM equals 10 nm, which is in very good agreement with the expected characteristics of the laser pulses.

The interference signal has modulation components with an oscillating period corresponding to the SH signal, i.e. a period of 1.2 fs. In order to obtain a good interference signal the stability level of the interferometer should be a fraction of this period, and moreover, hold for the entire integration time in each step. The delay fluctuations of the interferometer was measured with a HeNe laser to be ± 0.048 fs, which is well below the required stability.

In Fig. 5 the normalized surface FT-SHG spectrum of ZnO at approx. 60 K (line) and the frequency-doubled squared laser spectrum (dashed) obtained from the fundamental peak are displayed for laser pulses of 10 nm FWHM centered at 725±0.5 nm. The normalized FT-SHG spectrum is the ratio of seven averaged ZnO measurements and three averaged reference measurements on quartz. The bandwidth of the SHG signal is only measurable within the squared Gaussian intensity profile of the fs pulses as the SHG signal vanishes in noise towards the tails of the distribution. Hence, the spectral range has been cropped hereto. Clearly, a strong feature is seen around 3.413 eV, which

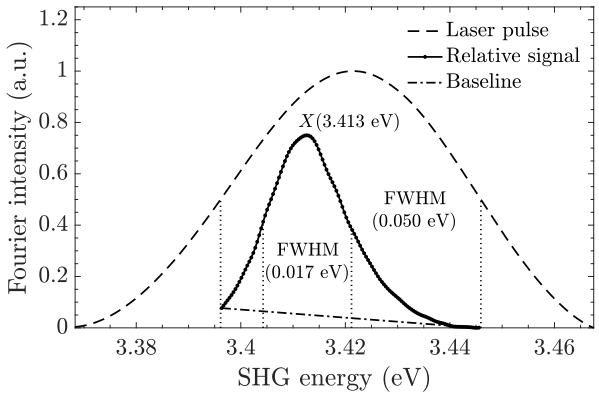

Figure 5: The relative SHG Fourier intensity of the ZnO and quartz wedge samples measured with 10 nm FWHM laser pulses centered at 725±0.5 nm

is in very good agreement with the strong exciton *X*-line observed at 3.407 eV in [10]. The 6 meV shift of the peak in SHG energy equals a wavelength shift of 0.6 nm. This is comparable to the laser stability of ±0.5 nm. However, the measurements were recorded at a temperature of approx. 60 K compared to 1.6 K in [10], which as well contributes to the shift. The FWHM of

the X-line in Fig. 5 is approximately 17 meV when the baseline is taken into account. According to [10], the magnitude of the X-line and the $1s_L(C)$ exciton decrease to approximately 20% at 50 K compared to the magnitude measured at 1.6 K, while the $2p_{x,y}(A)$ states vanish in the background above 30 K. Additionally, at 50 K the FWHM of the X-line and the $1s_L(C)$ exciton was observed to be roughly 2.2 times wider compared to the FWHM measured at 1.6 K [10]. The FWHM of the X-line can be estimated from [10] to be ~ 3 meV at 1.6 K resulting in a FWHM of ~ 7 meV at 50 K. Finally, Lafrentz *et. al.* observed that the peaks merge into one at 3.417 eV as the temperature rise to 128 K. In the view of this, we deduce that our measurements are consistent with those in [10].

Measurements of SHG from the ZnO and quartz wedge samples were also made without the Michelson interferometer using an Optical Parametric Amplifier (Light Conversion Topas-C Model 800-fs) pumped by 100 fs pulses of an amplified Ti:sapphire laser and a PMT at the exit of a monochromator was used as detector. Careful analysis of the spectra was necessary in order to separate SHG from strong two-photon photoluminescence generated at the band gap. Fig. 6 shows normalized SHG signal extracted from the measured spectra. The width of

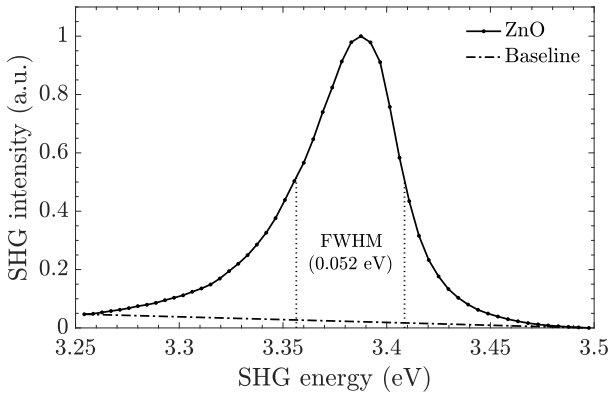

Figure 6: The normalized SHG signal of the ZnO wedge sample measured without the Michelson interferometer.

the peak is roughly 50 meV, which is three times larger than the exciton peaks detected with FT-SHG. Evidently, the use of fs laser pulses with the FT technique allows one to distinguish the narrow individual exciton resonance peaks.

4. Conclusion

We have shown that the spectral resolution in SHG spectroscopy using femtosecond laser pulses can be efficiently improved by the FT technique to achieve high spectral resolution independent of the input pulse characteristics. This was demonstrated by resolving the strong exciton X-line at 3.407 eV in ZnO, which is much narrower than the spectral bandwidth of femtosecond laser pulses used for excitation of the resonance. Furthermore, compared to conventional methods, our FT-SHG technique benefit the high spectral reproducibility of the FT approach due to built-in calibration of the spectral axis by Connes' advantage.

The presented method is enhanced if laser pulses with even broader spectral bandwidth are utilized to excite the sample. In this case a very broad spectral band can be covered in a single scan, while retaining high spectral resolution, without prolonging the scan duration.

5. Disclosures

Disclosures. The authors declare no conflicts of interest.

References

[1] Y. R. Shen, Wave mixing spectroscopy for surface studies, Solid State Communications 102 (2-3) (1997) 221–229. URL https://doi.org/10.1016/S0038-1098(96)00726-0

[2] D. R. Yakovlev, V. V. Pavlov, A. V. Rodina, R. V. Pisarev, J. Mund, W. Warkentin, M. Bayer, Exciton spectroscopy of semiconductors by the method of optical harmonics generation (review), Physics of the Solid State 60 (8) (2018) 1471–1486. URL https://doi.org/10.1134/S1063783418080231

[3] A. Prylepa, C. Reitböck, M. Cobet, A. Jesacher, X. Jin, R. Adelung, M. Schatzl-Linder, G. Luckeneder, K.-H. Stellnberger, T. Steck, J. Faderl, T. Stehrer, D. Stifter, Material characterisation with methods of nonlinear optics, Journal of Physics D: Applied Physics 51 (4) (2018) 043001. URL http://stacks.iop.org/0022-3727/51/i=4/a=043001

[4] D. A. Skoog, F. J. Holler, S. R. Crouch, Principles of Instrumental Analysis, 7th Edition, Cengage Learning, Boston, Massachusetts, 2018.

[5] J.-L. Coutaz, F. Garet, V. P. Wallace, Principles of Terahertz Time-Domain Spectroscopy, 1st Edition, Jenny Stanford Publishing, 2018.

[6] P. R. Griffths, J. A. de Haseth, Fourier Transform Infrared Spectrometry, 2nd Edition, John Wiley & Sons, Hoboken, New Jersey, 2007.

[7] A. P. Thorne, Fourier transform spectrometry in the ultraviolet, Analytical Chemistry 63 (2) (1991) 57A–65A. URL https://doi.org/10.1021/ac00002a712

[8] M. Bellini, A. Bartoli, T. W. Hänsch, Two-photon Fourier spectroscopy with femtosecond light pulses, Opt. Lett. 22 (8) (1997) 540–542. DOI:10.1364/OL.22.000540. URL http://ol.osa.org/abstract.cfm?URI=ol-22-8-540

[9] J. A. McGuire, W. Beck, X. Wei, Y. R. Shen, Fourier-transform sum-frequency surface vibrational spectroscopy with femtosecond pulses, Opt. Lett. 24 (24) (1999) 1877–1879. DOI:10.1364/OL.24.001877. URL http://ol.osa.org/abstract.cfm?URI=ol-24-24-1877

[10] M. Lafrentz, D. Brunne, A. V. Rodina, V. V. Pavlov, R. V. Pisarev, D. R. Yakovlev, A. Bakin, M. Bayer, Second-harmonic generation spectroscopy of excitons in ZnO, Phys. Rev. B 88 (2013) 235207. DOI:10.1103/PhysRevB.88.235207. URL https://link.aps.org/doi/10.1103/PhysRevB.88.235207

[11] J. Jerphagnon, S. K. Kurtz, Maker fringes: A detailed comparison of theory and experiment for isotropic and uniaxial crystals, Journal of Applied Physics 41 (4) (1970) 1667–1681. DOI:10.1063/1.1659090. URL https://doi.org/10.1063/1.1659090

[12] N. Bloembergen, P. S. Pershan, Light waves at the boundary of nonlinear media, Phys. Rev. 128 (1962) 606–622. DOI:10.1103/PhysRev.128.606. URL https://link.aps.org/doi/10.1103/PhysRev.128.606